This full text paper was peer reviewed at the direction of IEEE Communications Society subject matter experts for publication in the IEEE Globecom 2011 proceedings.

Joint Frequency Synchronization and Spectrum Occupancy Characterization in OFDM-based Cognitive Radio Systems

Milan Zivkovic, Rudolf Mathar
Institute for Theoretical Information Technology,
RWTH Aachen University
D-52056 Aachen, Germany
Email: {zivkovic,mathar}@ti.rwth-aachen.de

***Abstract*—OFDM-based cognitive radio (CR) systems are shown to be an effective solution for increasing spectrum efficiency by activating the certain group of subcarriers (subbands) in locally available spectrum. However, each CR receiver should synchronize itself to appropriate carrier frequency and to identify currently activated subbands. Moreover, energy and bandwidth efficiency of CR systems can be improved if each CR could provide additional characterization of the local spectral content. In this paper a novel joint frequency synchronization and spectrum occupancy characterization method for OFDM-based CR systems is proposed. The synchronization preamble structure is appropriately modified in order to efficiently perform frequency offset estimation, to identify occupied subbands, and, finally, to provide SNR and interference power estimates as reliable quantitative indicators of spectrum occupancy. The performance of proposed method is evaluated for different amounts of spectrum occupancy and interference levels.**

I. Introduction

Spectrum efficiency of current wireless systems can be significantly increased by opportunistic sharing of the available frequency band between licensed primary users (PU) and a group of unlicensed secondary users or cognitive radios (CRs) [1]. While monitoring the spectrum of interest, CRs are able to detect the unused portions (*spectrum holes*) and adapt waveform properties according to dynamically changing environment without introducing harmful interference to the PU. In order to regulate adaptive cooperative spectrum utilization, IEEE 802.22 working group initiated the standardization of wireless regional wireless networks (WRAN) for allowing broadband access in UHF/VHF TV bands between 54 and 862 MHz [2]. The standard also leaves the opportunity for extension of spectrum utilization methods within any regulatory regime.

Due to its flexibility in allocating resources among CRs, OFDM has been shown as a promising candidate for physical (PHY) layer in WRAN standard. OFDM is a multicarrier modulation scheme based on division of broadband channel into many narrowband subchannels modulated on different subcarriers. By leaving a set of subchannels unused, OFDM provides a flexible spectral shape that fills spectral gaps without interfering with the PU.

This work has been supported by the UMIC Research Center, RWTH Aachen University.

Standardization efforts for observation, decision, and action of CRs are widely discussed in [2]. One of them is based on fractional bandwidth (FBW) usage where common bandwidth is divided into several subbands which can be activated (occupied by CRs) if spectrum sensing indicates the absence of PUs within them. During the initialization, the OFDM CR receiver firstly needs to adjusts its timing, then to synchronize itself to appropriate carrier frequency and, finally, to identify active subbands in order to further process only the subcarriers which are belonging to them.

Therefore, after initial coarse timing estimation, the receiver has to estimate carrier frequency offset (CFO) which arises due to mismatch between transmitter's and receiver's oscillator. In most cases, the CFO may exceed the subcarrier spacing Δf. Therefore, it is customary to divide the CFO into an integer part (ICFO), a multiple of Δf which produces a shift of subcarrier indices, plus a fractional part (FCFO) which results into interchannel interference (ICI) due to loss of orthogonality among subcarriers. Conventional methods for estimating the fractional offset operate in the time-domain and measure the phase shift between the repetitive parts of a dedicated preambles [3]. In contrast, the integer offset is typically estimated in the frequency-domain by loading a known pseudo-noise (PN) sequence over used subcarriers [4]. This can be extended to mode detection as it is proposed in [5].

After the acquisition of carrier frequency, the identification of active subbands under FBW scenario can be reliably performed via a dedicated out-of-band control channel [6]. However, this approach can significantly reduce the bandwidth efficiency, particularly in heavy loaded networks, while increasing receiver complexity through the need of mutual synchronization among CR receivers. One efficient way to avoid the usage of control channel is to embed the information of currently used subbands into the structure of data packets. Authors in [5][6] utilize the synchronization preamble for embedding the information of spectrum usage patterns. Particularly, each CR identifies the FBW mode jointly with the ICFO estimation. However, those methods do not provide additional characterization of spectral content in order to quantify CR signal quality in active subbands and/or the level of interference in nonactive subbands. Such information can be further exploited for adapting transmission parameters (bandwidth, coding/data rate, power) in order to preserve

978-1-4244-9268-8/11/$26.00 ©2011 IEEE

energy and bandwidth efficiency of CR systems. A widely used standard measure of received signal quality is the signal-to-noise ratio (SNR). Under the FBW scenario, SNR in active subbands is defined as the ratio of the CR signal power to the noise power. Similarly, the level of interference in nonactive subbands can be characterized by interference power caused by the PU signal.

In this paper we utilize the time periodic structure of packet preamble proposed by [3] which allows for FCFO estimation over a wider CFO range with only one preamble, hence reducing the training symbol overhead. After FCFO is corrected, we modified the method proposed in [5] in order to exploit the general frequency domain form of the same preamble for joint ICFO estimation and current FBW mode detection. Moreover, we have shown in [7][8] that the given preamble structure can be also efficiently used for SNR estimation based on second order moments of received preamble samples. The key contribution of this paper is based on extension of our previous work which leads to robust and efficient SNR estimation in active subbands and interference power estimation in nonactive subbands under the FBW scenario, thus giving more detailed information on spectral content in this particular band.

Within the paper, the PU interference is modeled as additive Gaussian noise over subcarriers in nonactive subbands, as proposed in [9]. Additional assumption is that PU occupies all non active subbands with the same average power and that there is no mutual out of band transmission between PU and CR bands. Obtained results can be easily further extended by introducing filtering effects and arbitrary PU occupancy of the deactivated subbands.

The remainder of this paper is organized as follows. In Section II the FBW scenario is introduced and appropriate modification to synchronization preamble design is presented. The FCFO estimation proposed in [3] is briefly discussed under the FBW scenario in Section III, while the modifications assuming different number of time periodic parts for joint ICFO estimation and mode detection, proposed in [5], are considered in Section IV. The novel method for spectrum occupancy characterization by means of SNR estimation in detected active subbands and interference power estimation in nonactive subbands is described in Section V. The performance of proposed solution is analyzed by computer simulation in Section VI. Finally, some concluding remarks are drawn in Section VII.

II. System Model

A. Fractional Bandwidth (FBW) Scenario

As shown in Fig. 1, the FBW scenario assumes the opportunistic usage of common bandwidth B where PU signals can appear on preassigned portion of the band or dynamically change the position within it. After obtaining the information about spectrum occupancy provided by spectrum sensing, the CR transmitter deactivates (nulls) the subcarriers in the subbands occupied by PU signals. Moreover, by sensing any change in spectrum occupancy, the proposed CR system can activate previously nulled subbands or null the subbands that were active. As shown in Fig. 1, the common frequency band B, consisting of N subcarriers, is divided into $M = 8$ subbands, each carrying $N_{BW} = N/M$ subcarriers. The total number of activated subbands can vary from 1 to M where

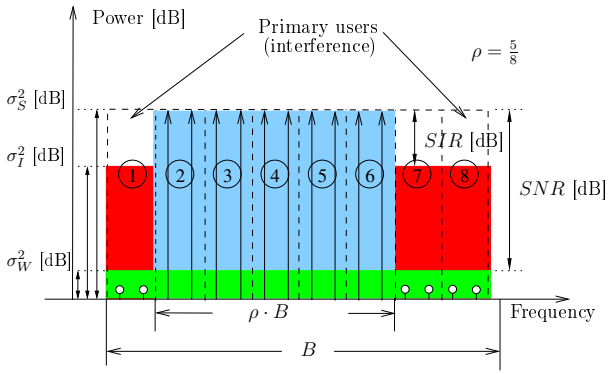

Fig. 1. Frequency representation of considered FBW model

only contiguous subbands are allowed to be activated in order to reduce the power leakage in the nulled subbands and mutual interference between PUs and CR [2]. Therefore, there are total $M_T = \frac{M(M+1)}{2}$ FBW modes with $M_A = 1, 2, \ldots, M$ contiguous active subbands.

Moreover, define *pool allocation* as $\rho = M_A/M$ as a parameter which indicates the level of CR system spectrum utilization [10]. In the example shown in Fig. 1, with $M = 8$ subbands, where the total $M_T = 36$ FBW modes are supported, currently $M_A = 5$ subbands are active, giving the pool allocation of $\rho = \frac{5}{8} = 0.625$.

B. Transmission model

The block diagram of typical CR system in FBW scenario is shown in Fig. 2. Given the spectrum sensing results, the CR transmitter activates particular FBW mode m by loading only the subcarriers of the active subbands of particular FBW mode while the rest of subcarriers is nulled. Let $C_m(n)$ denote the symbol carried on nth subcarrier in mode m, for $n = 0, \ldots, N-1$, while $\mathcal{S}_m$ present the set of subcarriers belonging to active subbands. Therefore,

$$C_m(n) = \begin{cases} S(n), & n \in \mathcal{S}_m \\ 0, & n \notin \mathcal{S}_m \end{cases}, \tag{1}$$

where $\sigma_S^2 = E\left\{|S(n)|^2\right\}$ is the average signal power. Without loss of generality, let's assume that all subcarriers in nonactive subbands are occupied with interference with same average power and that there is no interference power leakage to active subbands. The interference on subcarriers is modeled as sampled complex zero-mean Gaussian random variable with zero mean and variance σ_I^2, i.e., $I(n) \sim \mathcal{N}\left(0, \sigma_I^2\right)$ [9], thus giving

$$I_m(n) = \begin{cases} 0, & n \in \mathcal{S}_m \\ I(n), & n \notin \mathcal{S}_m \end{cases}. \tag{2}$$

Furthermore, noise samples are modeled as complex zero-mean AWGN, $W(n)$, with variance σ_W^2, i.e. $W(n) \sim \mathcal{N}\left(0, \sigma_W^2\right)$. To simplify the ongoing analysis, without losing generality, AWGN channel is considered, which is a regular assumption since timing synchronization is performed with sufficiently large cyclic prefix [6]. The spectral content on the subcarriers within the common bandwidth then can be written as

$$R(n) = \begin{cases} S(n) + W(n), & n \in \mathcal{S}_m \\ I(n) + W(n), & n \notin \mathcal{S}_m \end{cases}. \tag{3}$$

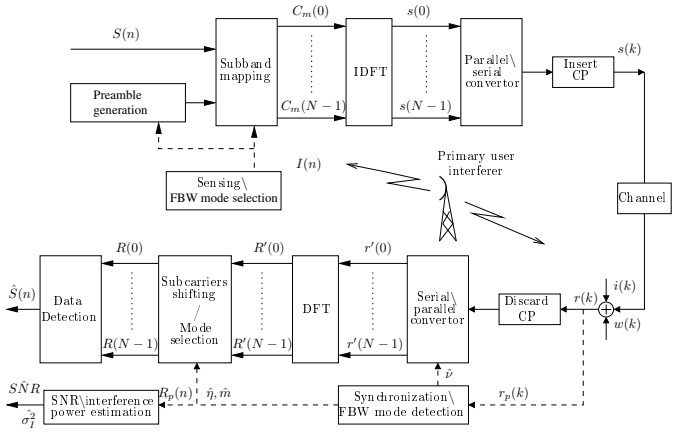

Fig. 2. The FBW system model

Therefore, we can define the frequency domain average signal-to-noise ratio (SNR) of the received signal in active subbands as

$$SNR = \frac{\sigma_S^2}{\sigma_W^2}. \tag{4}$$

Although desired signal and interference are separated within common band B, as shown in Fig. 1, let define the ratio between average signal power and average interference power as the average signal-to-interference ratio (SIR), written as

$$SIR = \frac{\sigma_S^2}{\sigma_I^2}. \tag{5}$$

The visual representation of above defined quantities and their relations in frequency domain is shown in Fig. 1.

In order to characterize received signal in time domain, let N_g denote the number of samples in cyclic prefix. At the receiver side the incoming signal after ADC is sampled at the rate $f_s = N\Delta f$, where Δf is the subcarrier spacing. Due to frequency mismatch between transmitter and receiver oscillator, the frequency f_{LO} of the local oscillator at the CR receiver differs from the received carrier frequency f_c. Let denote $\varepsilon = (f_c - f_{LO})/\Delta f$ the CFO normalized to the subcarrier spacing. Assuming the perfect timing synchronization, the received signal in time domain $r(k)$, for $k = -N_g, \ldots, N-1$, in the presence of normalized CFO ε, is given as

$$\begin{aligned} r(k) &= \frac{e^{\frac{j2\pi\epsilon k}{N}}}{N} \sum_{n=0}^{N-1} R(n) e^{-j2\pi \frac{nk}{N}} \\ &= \frac{e^{\frac{j2\pi\epsilon k}{N}}}{N} \Big(\big(\sum_{n\in\mathcal{S}_m} S(n) + \sum_{n\notin\mathcal{S}_m} I(n) \big) e^{-j2\pi \frac{nk}{N}} \Big) \\ &\quad + \frac{1}{N} \sum_{n=0}^{N-1} W(n) e^{-j2\pi \frac{nk}{N}} \\ &= e^{\frac{j2\pi\varepsilon k}{N}} \Big(s(k) + i(k) \Big) + w(k). \end{aligned} \tag{6}$$

We now give the insight into the preamble design issues in order to facilitate its time and frequency domain structure for joint CFO synchronization and spectrum occupancy characterization under the FBW scenario.

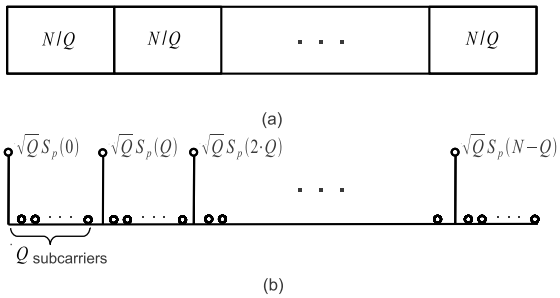

Fig. 3. Preamble structure in (a) time and (b) frequency domain

C. Preamble design

In many wireless OFDM systems, transmission is normally organized in frames where sequence of data symbols is preceded by several preambles of known data used for the synchronization and/or channel estimation purposes. Here we will use only one preamble with time periodic structure for FCFO estimation, joint ICFO estimation and mode detection, and, finally, for SNR and interference power estimation. We utilize the preamble structure proposed by Morelli and Mengali [3]. In order to cover a wider frequency range, preamble is divided into Q identical parts, each containing $N_p = N/Q$ samples as shown in Fig. 3. It can be also seen that such time periodic structure can be created in frequency domain by loading every Qth subcarrier.

Therefore, the time domain representation of the preamble with Q identical parts can be written as

$$s_p(k) = s_p(k + q\frac{N}{Q}),\ k = 0, \ldots, \frac{N}{Q} - 1,\ q = 1, \ldots, Q-1.$$

Given preamble can be formed in frequency domain by transmitting QPSK or PN sequence on every Qth subcarrier in the active subbands, thus giving

$$C_{p,m}(n) = \begin{cases} \sqrt{Q} S_p(n), & n \in \mathcal{S}_{p,m} \\ 0, & n \notin \mathcal{S}_{p,m} \end{cases}, \tag{7}$$

where $\mathcal{S}_{p,m}$ presents the set of loaded preamble subcarriers which belong to active subbands of mode m, i.e., $\mathcal{S}_{p,m} \subset \mathcal{S}_m$ while scaling factor $\sqrt{Q}$ is used to preserve average signal energy.

In order to perform joint ICFO estimation and mode detection using one preamble, authors in [4][5] proposed the differential coding structure of loaded subcarriers, which for given preamble with arbitrary number of time periodic parts Q, can be constructed as

$$S_p(n) = S_p(n-Q) \cdot P_m(n), n \in \mathcal{S}_{p,m} - N_{st,m}, \tag{8}$$

where $N_{st,m}$ is the index of the first carrier of mode m and P_m is the PN sequence used for embedding the information of particular mode m. Prior work [6][10] emphasized the advantage of using Frank-Zadoff-Chu (FZC) sequence due to its preferable autocorrelation properties and low PAPR behavior in time domain. Therefore, the FZC sequence used in (8) can be accommodated as [10]

$$P_m(n) = (-1)^{m\cdot n/Q} e^{\frac{j\pi m n^2}{\rho_m NQ}},\ n \in \mathcal{S}_{p,m}, \tag{9}$$

where ρ_m is the pool allocation for given mode m.

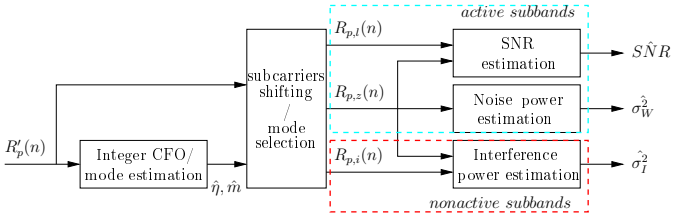

Fig. 4. Block diagram of the SNR and interference power estimator

Having this preamble structure, CFO can be decomposed into a fractional part ν which belongs to the interval $(-Q/2, Q/2]$, and an integer part which is a multiple of Q. Therefore, the normalized CFO can thus be written as

$$\varepsilon = \nu + \eta Q. \tag{10}$$

Clearly, the estimation of η is unnecessary if the maximum value of $|\varepsilon|$ is guaranteed to be less than $Q/2$, since in such a case we have $\eta = 0$.

III. Fractional CFO Estimation

Assume that the initial timing estimation was successfully performed utilizing the sufficiently large cyclic prefix [6], the next synchronization stage should then correct FCFO utilizing the time domain structure of received preamble. From (6), the received preamble in time domain, in the presence of normalized frequency offset ε can be written as

$$r_p(k) = e^{\frac{j2\pi\varepsilon k}{N}}(s_p(k) + i_p(k)) + w_p(k). \tag{11}$$

Authors in [3] proposed the best linear unbiased estimator (BLUE) of FCFO which is given as

$$\hat{\nu} = \frac{Q}{2\pi}\sum_{j=1}^{Q/2} w(j)\varphi(j) \tag{12}$$

where

$$w(j) = \frac{12(Q-j)(Q-j+1) - 3Q^2}{2Q(Q^2-1)}, \tag{13}$$

and $\varphi(j)$ is the angle

$$\varphi(j) = \left[\arg\left\{\frac{V(j)}{V(j-1)}\right\}\right]_{2\pi}. \tag{14}$$

Here $[x]_{2\pi}$ presents modulo 2π operation and $V(j)$ denotes the correlation of time periodic preamble parts separated by jN/Q samples given as

$$V(j) = \frac{1}{N - jN/Q}\sum_{k=jN/Q}^{N-1} r_p(k)r_p^*(k - j\frac{N}{Q}),\ \ 0 \le j \le Q/2.$$

After obtaining the FCFO estimate $\hat{\nu}$, the phase corrected preamble samples $r'_p(k)$ signal can be written as

$$r'_p(k) = r_p(k)e^{-\frac{j2\pi\hat{\nu}k}{N}}. \tag{15}$$

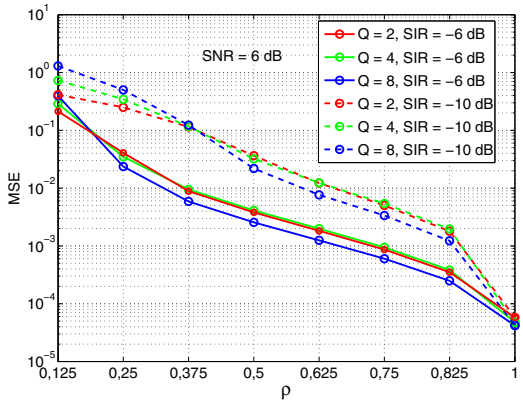

Fig. 5. MSE vs. pool allocation for SNR = 6 dB at SIR = -6 dB and -10 dB

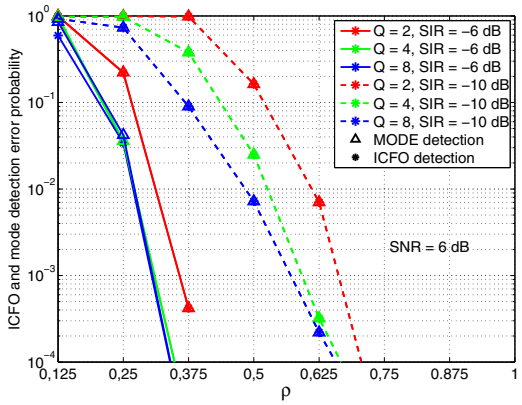

Fig. 6. ICFO and mode detection error probability vs. pool allocation for SNR = 6 dB at SIR = -6 dB and -10 dB

IV. Joint Integer CFO and FBW Mode Estimation

Assuming perfect FCFO compensation, i.e., $\hat{\nu} = \nu$, the frequency domain form of of phase corrected preamble $R'_p(n) = \text{IFFT}_N[r'_p(k)]$ will be shifted due to the ICFO presence, thus giving

$$R'_p(n) = \begin{cases} \sqrt{Q}S_p(|n-\eta Q|_N)P_m(|n-\eta Q|_N) + W(n), & n \in \mathcal{S}_{p,m,\eta Q} \\ W(n), & n \in \mathcal{S}_{p,z,\eta Q} \\ I(|n-\eta Q|_N) + W(n), & n \in \mathcal{S}_{p,i,\eta Q} \end{cases}$$

where $|n-\eta Q|_N$ is the value $n-\eta Q$ reduced to the interval $[0, N-1]$. Here, $\mathcal{S}_{p,m,\eta Q}$ is the set of subcarriers where CR signal is present and which satisfy $\Big((n \in \mathcal{S}_{p,m}) \wedge (|n-\eta Q|_N \le \rho N + N_{st,m} - n)\Big) \vee \Big((n \notin \mathcal{S}_m) \wedge (|n-\eta Q|_N > \rho N + N_{st,m} - n) \wedge ([|n - N_{st,m}|]_Q = 0)\Big)$. Similarly, $\mathcal{S}_{p,z,\eta Q}$ present the set of subcarries with only noise samples for which holds $\Big((n \in \mathcal{S}_{z,m}) \wedge (|n-\eta Q|_N \le \rho N + N_{st,m} - n)\Big) \vee \Big((n \notin \mathcal{S}_m) \wedge (|n-\eta Q|_N > \rho N + N_{st,m} - n) \wedge ([|n - N_{st,m}|]_Q \ne 0)\Big)$, where $\mathcal{S}_{z,m}$ denote the set of nulled subcarriers which belong to active subbands of mode m, thus $\mathcal{S}_{z,m} = \mathcal{S}_m / \mathcal{S}_{p,m}$. Further, $\mathcal{S}_{p,i,\eta Q}$ is the set of subcarriers where interfering PU signal is present and which satisfy $\Big((n \notin \mathcal{S}_m) \wedge (|n-\eta Q|_N \le \rho N + N_{st,m} - n)\Big) \vee \Big((n \in \mathcal{S}_m) \wedge (|n-\eta Q|_N > \rho N + N_{st,m} - n)\Big)$.

Utilizing the structure of appropriately constructed preamble defined in (7), the ICFO η and current mode m can be

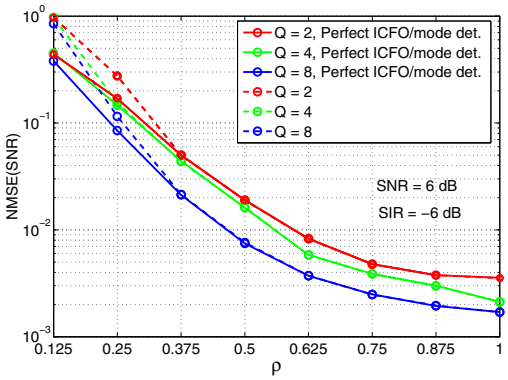

Fig. 7. NMSE(SNR) vs. pool allocation for SNR = 6 dB and SIR = -6 dB

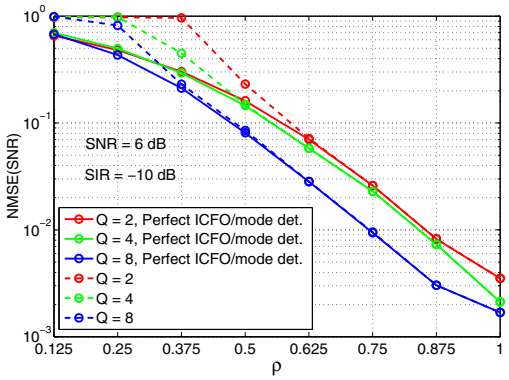

Fig. 8. NMSE(SNR) vs. pool allocation for SNR = 6 dB and SIR = -10 dB

estimated by maximizing the following differential correlation [5][6]

$$B_m(\hat{\eta})=\frac{|\sum_{n\in\mathcal{S}_{p,m}} R'_p(n+\eta Q)R'^{*}_p(n+\eta Q+Q)P_m(n+Q)|^2}{(\sum_{n\in\mathcal{S}_{p,m}}|R'_p(n+\eta Q)|^2)^2}, \tag{16}$$

which yields appropriate estimates

$$(\hat{m},\hat{\eta}) = \arg\max_{(m,\eta)} |B_m(\hat{\eta})|^2, \tag{17}$$

for $1 \le m \le M_T$.

V. SNR and Interference Power Estimation

Given the ICFO estimation and mode detection obtained in (17), the spectral content characterization can be performed by means of SNR estimation in active subbands and interference power estimation in nonactive subbands. After shifting the received signal $R'_p(n)$ with estimated ICFO $\hat{\eta}$, the corrected signal can be written as

$$R_p(n) = R'_p(n+\hat{\eta}Q). \tag{18}$$

Assuming perfect FCFO and ICFO estimation and mode detection, i.e. $\hat{\nu}=\nu$, $\hat{\eta}=\eta$, and $\hat{m}=m$, respectively, the received preamble can be written as

$$R_p(n) = \begin{cases} R_{p,l}(n), & n \in \mathcal{S}_{p,m} \\ R_{p,z}(n), & n \in \mathcal{S}_{z,m} \\ R_{p,i}(n), & n \notin \mathcal{S}_m, \end{cases} \tag{19}$$

where

$$R_{p,l}(n) = \sqrt{Q}S_p(n)P_m(n) + W(n) \tag{20}$$

denotes the received signal on loaded subcarriers of active mode m. Further,

$$R_{p,z}(n) = W(n) \tag{21}$$

denotes the received signal on nulled subcarriers of active mode m, and

$$R_{p,i}(n) = I(n) + W(n) \tag{22}$$

is the received signal in nonactive subband.

Extending the preamble-based method for average SNR estimation that authors proposed in [7][8], the empirical second-order moment of the received signal on loaded subcarriers in active subbands can be written as

$$\hat{M}_{2,l} = \frac{Q}{\rho N}\sum_{n\in\mathcal{S}_{p,m}} |R_{p,l}(n)|^2, \tag{23}$$

with expected value $E\{\hat{M}_{2,l}\} = Q\sigma_S^2 + \sigma_W^2$. Similarly, the empirical second-order moment of the received signal on nulled subcarriers in active subbands, given as

$$\hat{M}_{2,z} = \frac{Q}{\rho N(Q-1)}\sum_{n\in\mathcal{S}_{z,m}} |R_{p,z}(n)|^2, \tag{24}$$

has expectation $E\{\hat{M}_{2,z}\} = \sigma_W^2$. Finally, the empirical second-order moment of the received signal on subcarriers in nonactive subbands is given as

$$\hat{M}_{2,i} = \frac{1}{(1-\rho)N}\sum_{n\notin\mathcal{S}_m} |R_{p,i}(n)|^2 \tag{25}$$

with expected value $E\{\hat{M}_{2,i}\} = \sigma_I^2 + \sigma_W^2$.

As shown in [7][8], the average SNR can be estimated as

$$\begin{aligned} \hat{SNR} &= \frac{1}{Q}\frac{\hat{M}_{2,l}-\hat{M}_{2,z}}{\hat{M}_{2,z}} \\ &= \frac{1}{Q}\Big((Q-1)\frac{\sum_{n\in\mathcal{S}_{p,m}}|R_{p,l}(n)|^2}{\sum_{n\in\mathcal{S}_{z,m}}|R_{p,z}(n)|^2}-1\Big), \end{aligned} \tag{26}$$

where, by the strong law of large numbers, $\hat{M}_{2,l}$ and $\hat{M}_{2,z}$ are strongly consistent unbiased estimators of $QS+W$ and average noise power W, respectively. Similarly, the interference power σ_I^2 can be estimated as

$$\begin{aligned} \hat{\sigma_I^2} &= \hat{M}_{2,i} - \hat{M}_{2,z} \\ &= \frac{1}{N}\Big(\frac{1}{1-\rho}\sum_{n\notin\mathcal{S}_m}|R_{p,i}(n)|^2 - \frac{Q}{\rho(Q-1)}\sum_{n\in\mathcal{S}_{z,m}}|R_{p,z}(n)|^2\Big). \end{aligned} \tag{27}$$

The block diagram of proposed estimators is shown in Fig. 4

VI. Performance Evaluation

The performance of proposed preamble-based joint frequency estimation and spectrum occupancy characterization method in cognitive radio systems under the FBW scenario is evaluated using Monte-Carlo simulation. It is assumed that timing synchronization is already performed while the CR channel is considered as AWGN, which is a regular assumption since the cyclic prefix is sufficiently large. However, the straightforward extension to other types of channels can be conducted. It is further assumed that the total number of subcarriers is 1024 according to WRAN standard [2].

The available band is divided into $M = 8$ subbands, where the lowest mode corresponds to pool allocation $\rho = 0.125$,

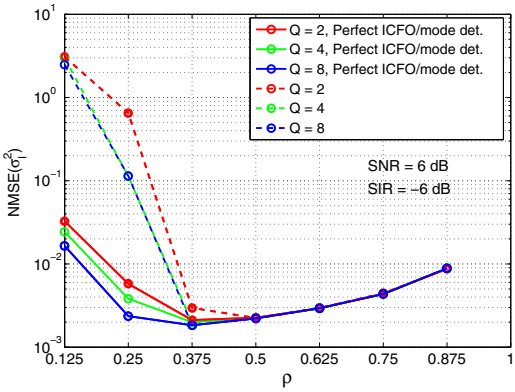

Fig. 9. NMSE(σ_I^2) vs. pool allocation for SNR = 6 dB and SIR = -6 dB

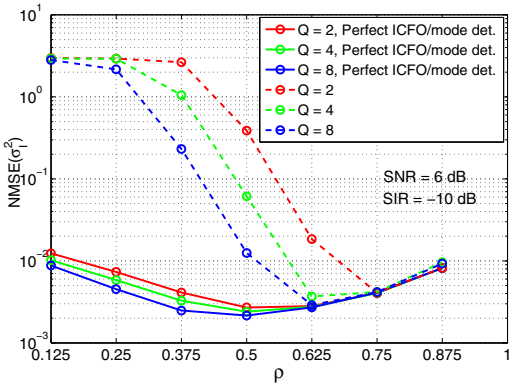

Fig. 10. NMSE(σ_I^2) vs. pool allocation for SNR = 6 dB and SIR = -10 dB

while the highest mode, where $\rho = 1$, corresponds to the absence of PU when CR occupies the whole band. Different number of time periodic parts, i.e., $Q = 2, 4$, and 8 is considered for analysis. Furthermore, the normalized CFO is taken to be $\varepsilon = 8.5$, which corresponds to $\nu = 0.5$ and $\eta = 4, 2$, and 1 for $Q = 2, 4$, and 8, respectively. The accuracy of the FCFO estimation is measured in terms of mean square error (MSE), which is defined as $E\{|\hat{\mu} - \mu|^2\}$. Fig. 5 shows the performance of MSE vs. ρ for $Q = 2, 4$, and 8. The SIR is chosen to be -6 and -10 dB while SNR is fixed at 6 dB. It can be seen that MSE decreases with ρ and that for both SIR values there are slight variations of MSE with respect to Q.

The ICFO and mode detection error probabilities, defined as $\Pr(\hat{\eta} \neq \eta)$ and $\Pr(\hat{m} \neq m)$, respectively, are shown in Fig. 6. Since they are obtained from joint maximization of differential correlation defined in (16), their performance overlap along all considered values of given parameters. It can be also seen that for SIR = -6 dB, the cases when $Q = 4, 8$ perform almost the same and outperform the case when $Q = 2$ while the error probabilities go below 10^{-3} even for the $\rho = 0.375$. Similarly, for SIR = -10 dB the error probabilities are smaller than 10^{-3} starting from $\rho = 0.625$ and $\rho = 0.75$ for $Q = 4, 8$ and $Q = 2$, respectively.

The SNR estimation is evaluated in terms of normalized MSE, or NMSE(SNR), defined as $E\{(\frac{\hat{SNR}-SNR}{SNR})^2\}$, while NMSE($\sigma_I^2$), defined as $E\{(\frac{\hat{\sigma_I^2}-\sigma_I^2}{\sigma_I^2})^2\}$, is used as performance measure for interference power estimation. Fig. 7 and Fig. 8 show NMSE(SNR) vs. ρ for fixed SNR = 6 dB and SIR = -6 dB and SIR = -10 dB, respectively. Two cases are analyzed here: the first case considers the perfect ICFO estimation and mode detection while the second case assumes that those estimates are jointly obtained using (17). As it is expected, the increase of Q improves performance. For SIR = -6 dB the performance of both cases overlaps starting from $\rho = 0.375$ which agrees to detection error performance depicted in Fig. 6. Similar behavior can be noticed for SIR = -10 dB.

Fig. 9 and Fig. 10 shows NMSE(σ_I^2) vs. ρ performance for the same set of parameters which are considered in SNR estimation analysis. As it is expected, the increase of Q improves performance due to increased number of available noise samples in active subbands, thus making (24) more accurate. Additionally, when ρ increases, there are two opposite effects which influence the performance, since for both SIR values there is a certain value of ρ up to which NMSE(σ_I^2) decreases while afterwards increases. This can be explained with the change of the number of available samples which determine the accuracy of estimates $\hat{M}_{2,i}$ and $\hat{M}_{2,z}$, defined in (24) and (25), respectively. It can be seen that this value is additionally determined by the actual SIR value and, in contrast to SNR estimation, is shown to be very sensitive to previously performed ICFO estimation and mode detection.

VII. Conclusion

In this paper, we propose a novel joint frequency synchronization and spectrum occupancy characterization method for OFDM-based CR systems under FBW scenario. The synchronization preamble structure is appropriately modified and utilized for efficient frequency offset estimation, for identification of occupied subbands, and, finally, for SNR and interference power estimation considered as quantitative measure of the spectral content. The performance of proposed approach is evaluated for different amounts of spectrum occupancy and interference levels. Simulation results show that the increase of time periodic parts of synchronization preamble improves performance of proposed method and that SNR estimation performs well even for low spectrum occupancy. On the contrary, interference power estimation is more sensitive to residual errors originating from carrier frequency estimation and mode detection, especially for low spectrum occupancy.

References

[1] I. Mitola, J. and J. Maguire, G.Q., "Cognitive radio: making software radios more personal," *IEEE Pers. Commun.*, vol. 6, no. 4, pp. 13–18, Aug. 1999.

[2] J. Benko, S.-Y. Chang, and Y.-C. Cheong, "Draft PHY/MAC specification for IEEE 802.22," IEEE 802.22-06/0069r1, Tech. Rep., 2006.

[3] M. Morelli and U. Mengali, "An improved frequency offset estimator for OFDM applications," *IEEE Commun. Lett.*, vol. 3, no. 3, pp. 75–77, Mar 1999.

[4] Y. H. Kim, I. Song, S. Yoon, and S. R. Park, "An efficient frequency offset estimator for OFDM systems and its performance characteristics," *IEEE Trans. Veh. Technol.*, vol. 50, no. 5, pp. 1307 –1312, Sep. 2001.

[5] J. Y. Won, H. G. Kang, Y. H. Kim, I. Song, and M. S. Song, "Fractional bandwidth mode detection and synchronization for OFDM-based cognitive radio systems," *Proc. of IEEE VTC 2008 Spring*, pp. 1599 –1603, 2008.

[6] S. Feng, H. Zheng, H. Wang, J. Liu, and P. Zhang, "Preamble design for non-contiguous spectrum usage in cognitive radio networks," in *Proc. of IEEE WCNC'09*, ser. WCNC'09.

[7] M. Zivkovic and R. Mathar, "Preamble-based SNR estimation in frequency selective channels for wireless OFDM systems," *Proc. of IEEE VTC 2009 Spring*, 2009.

[8] ——, "An improved preamble-based SNR estimation algorithm for OFDM systems," *Proc. of IEEE PIMRC 2010, Istanbul, Turkey*, pp. 172 –176, 2010.

[9] T. Yucek and H. Arslan, "MMSE noise plus interference power estimation in adaptive OFDM systems," *IEEE Trans. Veh. Technol.*, vol. 56, no. 6, pp. 3857 –3863, Nov. 2007.

[10] M. Krondorf, T.-J. Liang, and G. Fettweis, "On synchronization of opportunistic radio OFDM systems." *Proc. of IEEE VTC 2008 Spring*, pp. 1686–1690, 2008.